Cosmic Tidal Reconstruction

Hong-Ming Zhu,[1,2] Ue-Li Pen,[3,4,5] Yu Yu,[6] Xinzhong Er,[1,7] and Xuelei Chen[1,8]

[1]*Key Laboratory for Computational Astrophysics, National Astronomical Observatories, Chinese Academy of Sciences, 20A Datun Road, Beijing 100012, China*
[2]*University of Chinese Academy of Sciences, Beijing 100049, China*
[3]*Canadian Institute for Theoretical Astrophysics, 60 St. George Street, Toronto, ON M5S 3H8, Canada*
[4]*Canadian Institute for Advanced Research, CIFAR Program in Gravitation and Cosmology, Toronto, ON M5G 1Z8, Canada*
[5]*Perimeter Institute for Theoretical Physics, 31 Caroline St. N., Waterloo, ON, N2L 2Y5, Canada*
[6]*Key laboratory for research in galaxies and cosmology, Shanghai Astronomical Observatory, Chinese Academy of Science, 80 Nandan Road, Shanghai 200030, China*
[7]*INAF, Osservatorio Astronomico di Roma, via Frascati 33, I-00040, Monteporzio Catone, Italy*
[8]*Center of High Energy Physics, Peking University, Beijing 100871, China*

(Dated: November 5, 2015)

The gravitational interaction of a long wavelength tidal field with small scale density fluctuations leads to anisotropic distortions of the local two point correlation function. Since the correlation function is known to be statistically isotropic in the absence of tidal interactions, the tidal distorted parts can be used to reconstruct the long wavelength tidal field in analogy with lensing of the CMB. In this paper we show that these distortions can be reconstructed and used to probe the large scale distribution of dark matter in the Universe. The plentiful information encoded in the small scale structures allows accurate reconstruction of the matter density field on large scales, $k \lesssim 0.1h$/Mpc. We perform cosmic tidal reconstruction in N-body simulations and find the cross correlation coefficient between the reconstructed field and the original density field is above 0.8 and close to 0.9 on some scales. This helps the reconstruction of radial modes lost in 21cm intensity mapping surveys.

PACS numbers:

I. INTRODUCTION

The large scale structure contains a wealth of information about our Universe. The cosmic acceleration, neutrino masses, early universe models and a lot of other properties of the Universe can be learned with current or upcoming surveys. From what we have already learned, the initial density perturbations have small amplitudes and nearly Gaussian distributions with different Fourier modes independent with each other, these grow due to gravitational interaction, nonlinearities developed and couplings between different modes were induced. This leads to striking non-Gaussian features in the present large scale structure of the Universe, limiting the cosmological information that can be extracted from galaxy surveys. At the same time, however, such correlations between the different perturbation modes on different scales also imply that we could infer a lot about the large scale density field by observing small scale density fluctuations.

The basic idea of such reconstruction is that the evolution of small scale density perturbations $\boldsymbol{k}_S$ are modulated by a long wavelength perturbation $\boldsymbol{k}_L$, causing both isotropic and anisotropic distortions of the local power spectrum [1]. The isotropic distortion, which depends only on the magnitude of the wavenumber $\boldsymbol{k}_S$, is mainly due to the change in the background density from the long wavelength density perturbation $\nabla^2\Phi_L \propto \delta_L$. The anisotropic distortion, which also depends on the direction of $\boldsymbol{k}_S$, is induced by the long wavelength tidal field $t_{ij} = \Phi_{L,ij} - \delta_{ij}\nabla^2\Phi_L/3$. Using the isotropic modulation on the small scale power spectrum to recover the large scale density field were studied in Ref.[2]. ue-li can you add something about Bond's work here? I'm not very clear what they have done. However, the anisotropic distortions are more robust, since many other processes can also lead to isotropic distortions in the local small scale power spectrum. By applying quadratic estimators which quantify the local anisotropy of small scale filamentary structures, the long wavelength tidal field can be reconstructed accurately [3]. In general, this method can be applied to obtain measurement of long wavelength modes with better precision, this is especially valuable when these modes can not be obtained directly. The reconstruction of the long wavelength tidal field from the distorted local power spectrum is similar to the reconstruction of shear fields in gravitational lensing [4, 5].

In this paper we present the cosmic tidal reconstruction method in detail. The evolution of small scale density fluctuations in the presence of the long wavelength tidal field t_{ij} has been studied extensively in Ref.[1]. The tidal distorted parts in the local small scale power spectrum is given by

$$\delta P(\boldsymbol{k}_S,\tau)|_{t_{ij}} = \hat{k}_S^i \hat{k}_S^j t_{ij}^{(0)} P_{1s}(k_S,\tau) f(k_S,k_L,\tau), \qquad (1)$$

where $\hat{\boldsymbol{k}}$ denotes the unit vector in the direction of $\boldsymbol{k}$, $P_{1s}(k_S,\tau)$ is the isotropic linear power spectrum, $f(k_S,k_L,\tau)$ describes the coupling of the long wavelength tidal field to the small scale density fluctuations and superscript (0) denotes some "initial" time. The

anisotropic distortion can be decomposed into sevaral orthogonal quadrupolar distortions if we write t_{ij} in the following form:

$$t_{ij} = \begin{pmatrix} \gamma_1 - \gamma_z & \gamma_2 & \gamma_x \\ \gamma_2 & -\gamma_1 - \gamma_z & \gamma_y \\ \gamma_x & \gamma_y & 2\gamma_z \end{pmatrix}. \quad (2)$$

We are interested in two transverse shear terms $(\hat{k}_1^2 - \hat{k}_2^2)\gamma_1^{(0)} P_{1s} f$ and $2\hat{k}_1\hat{k}_2\gamma_2^{(0)} P_{1s} f$, which describe orthogonal quadrupolar distortions in the tangential plane perpendicular to the line of sight, while the quadrupolar distortions concerning $\hat{k}_3$ will be affected by peculiar velocities. Here $\gamma_+ = (\Phi_{L,11} - \Phi_{L,22})/2$ and $\gamma_\times = \Phi_{L,12}$. These two tidal shear fields can be converted into the 2D convergence field $\kappa_{2D} = (\Phi_{L,11} + \Phi_{L,22})/2$ using $\kappa_{2D,11} + \kappa_{2D,22} = \gamma_{+,11} - \gamma_{+,22} + 2\gamma_{\times,12}$. We can obtain the 3D convergence field $\kappa_{3D} = \nabla^2\Phi_L/3$ from $\kappa_{3D,11} + \kappa_{3D,22} = 2\nabla^2\kappa_{2D}/3$. The large scale density field δ_L is given by the 3D convergence field through the Poisson equation. Here the two tidal shear fields are evaluated by applying quadratic estimators to the density field as in weak lensing. The optimal tidal shear estimators can be derived under the Gaussian assumption.

We call this method *cosmic tidal reconstruction*, as it exploits the local tidal distorted anisotropic features. Each independent measurement of the small scale power spectrum gives some information about the power spectrum on longer linear scales. Thus instead of being limited by the non-Gaussianity on small scales, we exploit these strong correlations to improve the measurement of the large scale structure.

Since we only use the tidal shear fields in the $x-y$ plane to reconstruct the long wavelength density field, the change of long wavelength density field δ_L along z axis is inferred from the variations of tidal shear fields γ_1 and γ_2 along z axis. We can not capture rapid changes of the density field along z axis, i.e. those modes with large $k_\parallel$. The noise of the reconstructed mode $\kappa_{3D}(\boldsymbol{k})$ is

$$\sigma^2_{\kappa_{3D}} \propto \left(\frac{k^2}{k_\perp^2}\right)^2, \quad (3)$$

where the anisotropic dependence is due to we only use γ_1 and γ_2 to reconstruct the large scale density field. The noise is infinite when $k_\perp \to 0$. In this case, we expect these modes contain nothing but noise. The well reconstructed modes are those with small $k_\parallel$ and large $k_\perp$. This helps the correlation of 21cm intensity mapping survey with other cosmic probes ... ue-li can you add something here?

The local quadrupolar distortions have also been discussed in [6].ue-li can you also add something here?

The remaining part of this paper is organized as follows. In Section II, we present the basic formalism, including kinematics, dynamics, reconstruction algorithm and tidal shear estimators. In Section III, we study cosmic tides in N-body simulations. In Section IV, we examine the validity of cosmic tidal reconstruction and discuss its future applications.

II. TIDAL DEFORMATION

The motion of a dark matter fluid element in the Universe includes translation, rotation and deformation. Let us consider two neighboring points P_0 and P in the fluid at time t_0, the velocity $\boldsymbol{v}|_P$ can be expanded as

$$v^i|_P = v^i|_{P_0} + (S^i{}_j + A^i{}_j)|_{P_0}\Delta x^j. \quad (4)$$

where the symmetric part $S^i{}_j = (v^i{}_{,j} + v_j{}^{,i})/2$ is the deformation velocity tensor in fluid mechanics, with diagonal components describing the stretching along three axises and off-diagonal components describing the shear motion; the anti-symmetry part $A^i{}_j = (v^i{}_{,j} - v_j{}^{,i})/2$ describes the rotation of this fluid element. In the free falling reference system of this fluid element, $v|_{P_0} = 0$. Neglecting the rotation, the position of P at time t is given by

$$\Delta x^i(t)|_P = \Delta x^i_0 + \int_{t_0}^{t} S^i{}_j(t')|_{P_0} dt' \Delta x^j_0, \quad (5)$$

where Δx^i_0 is the initial separation between P_0 and P. The shape tensor $\mathfrak{S}^i{}_j = \int_{t_0}^t S^i{}_j(t')|_{P_0} dt'$ describes the deformation. In the local inertial frame, the free falling dark matter fluid elements are only sensitive to the residual gravitational forces, similar to the ocean tides on Earth induced by the tidal forces from the Moon and the Sun. We call such effects by the surrounding large scale structure *cosmic tides*. The observable structures of baryonic tracers will also exhibit the same local anisotropies. The long wavelength tidal field and the large scale density may then be inferred from observation. In reality, the interaction between the long wavelength tidal field and small scale density fluctuations is more complicated than the displacement of particles in a fluid element, we shall discuss this in more detail below.

In the expanding universe, the equation of motion for a particle is

$$\frac{d^2\boldsymbol{x}}{d\tau} + \mathcal{H}(\tau)\frac{d\boldsymbol{x}}{d\tau} = -\nabla_{\boldsymbol{x}}\phi, \quad (6)$$

where $\boldsymbol{x}$ is the comoving Eulerian coordinate, τ is the conformal time, $\mathcal{H} = d\ln a(\tau)/d\tau$ is the comoving Hubble parameter, $a(\tau)$ is the scale factor and ϕ is the gravitational potential. In Lagrangian perturbation theory, the dynamical variable is the Lagrangian displacement field $\mathbf{s}(\boldsymbol{q}, \tau)$, defined as

$$\boldsymbol{x}(\tau) = \boldsymbol{q} + \mathbf{s}(\boldsymbol{q}, \tau), \quad (7)$$

where $\boldsymbol{q}$ is the comoving Lagrangian coordinate. The displacement field maps the initial particle position $\boldsymbol{q}$ into

the final Eulerian position $\boldsymbol{x}$. The density contrast $\delta(\boldsymbol{x})$ is given by the mass conservation relation:

$$\delta(\boldsymbol{x}(\boldsymbol{q},\tau)) = \det(\delta^i{}_j + \mathrm{M}^i{}_j(\boldsymbol{q},\tau)) - 1 \tag{8}$$

where $\mathrm{M}^i{}_j = \partial \mathrm{s}^i/\partial q^j$.

To study the evolution of small scale density perturbations in the presence of the long wavelength tidal field, we decompose the gravitational potential ϕ into a part sourced by the small scale density fluctuations, Φ_s and a part induced by the long wavelength tidal field up to second order,

$$\phi(\boldsymbol{x}(\boldsymbol{q},\tau)) = \Phi_s(\boldsymbol{x}(\boldsymbol{q},\tau)) + \frac{1}{2}t_{kl}(\boldsymbol{0},\tau)x^k x^l + ... \tag{9}$$

The tidal field can be written as $t_{ij}(\boldsymbol{0},\tau) = T(\tau)t^{(0)}_{ij}(\boldsymbol{0})$, where superscript (0) denotes the tidal field evaluated at the "initial" time τ_0, $T(\tau) = D(\tau)/a(\tau)$ is the transfer function, which is independent of wavelength during the linear growth stage, $D(\tau)$ is the linear growth function, $D(\tau_0) = a(\tau_0) = 1$. Note that at the origin of the free falling frame, the contribution from the tidal field is by definition zero. The small scale potential Φ_s satisfies the Poisson equation,

$$\nabla^2\Phi_s = 4\pi G a^2\bar{\rho}\delta = \frac{3}{2}\Omega_m(\tau)\mathcal{H}^2\delta, \tag{10}$$

where $\Omega_m(\tau)$ is the density parameter at τ.

The above equations could be solved perturbatively. We decompose the displacement as

$$\mathbf{s} = \mathbf{s}_s + \mathbf{s}_t, \tag{11}$$

where $\mathbf{s}_s$ and $\mathbf{s}_t$ are the contributions from the small scale local potential and long wavelength tidal field respectively. Then $\mathrm{M}^i{}_j = \mathrm{M}_s{}^i{}_j + \mathrm{M}_t{}^i{}_j$ with $\mathrm{M}_s{}^i{}_j = \partial \mathrm{s}^i_s/\partial q^j$, $\mathrm{M}_t{}^i{}_j = \partial \mathrm{s}^i_t/\partial q^j$. Here we only consider the linear displacement $\mathbf{s}_{1s}$, $\mathbf{s}_{1t}$ and the quadratic term $\mathbf{s}_{2t}$ from the coupling of $\mathbf{s}_{1s}$ and $\mathbf{s}_{1t}$, and neglect the terms of order $(\mathbf{s}_{1s})^2$, which are nonlinear interaction between small scale modes. In the follow calculations, we focus on the coupling between the long mode (large scale tidal field) and the short mode (small scale density field), assuming that both large and small scale density fields underwent linear evolutions.

At linear order, Eq.(6) becomes two equations for $\mathbf{s}_{1s}$ and $\mathbf{s}_{1t}$, respectively,

$$\begin{aligned}\left[\frac{d^2}{d\tau^2} + \mathcal{H}\frac{d}{d\tau}\right]\mathrm{s}^i_{1s}(\boldsymbol{q},\tau) &= -\partial^i_q\Phi_{1s}(\boldsymbol{q},\tau),\\ \left[\frac{d^2}{d\tau^2} + \mathcal{H}\frac{d}{d\tau}\right]\mathrm{s}^i_{1t}(\boldsymbol{q},\tau) &= -\frac{1}{2}\partial^i_q[t_{kl}(\tau)q^k q^l],\end{aligned} \tag{12}$$

where $\partial^i_q \equiv \delta^{ij}\partial/\partial q^j$, and $\nabla^2_q\Phi_{1s} = 3\Omega_m(\tau)\mathcal{H}^2\delta_{1s}/2$, $\delta_{1s} = -\mathrm{s}^i_{1s,i}$. Should add more detail here.

The first equation can be solved to get

$$\mathrm{s}^i_{1s}(\boldsymbol{q},\tau) = -\frac{\partial^i_q}{\nabla^2_q}\delta_{1s}(\boldsymbol{q},\tau) = -D(\tau)\frac{\partial^i_q}{\nabla^2_q}\delta_{1s}(\boldsymbol{q},\tau_0). \tag{13}$$

where we use $\frac{1}{\nabla^2}$ to denote the inverse operator for ∇^2, which can be easily computed in Fourier space. The second equation which describes the evolution of the displacement induced by the long wavelength tidal field can be integrated to get

$$\mathrm{s}^i_{1t}(\boldsymbol{q},\tau) = -F(\tau)t^{(0)i}{}_j q^j, \tag{14}$$

where

$$F(\tau) = \int_0^\tau d\tau'' a(\tau'')T(\tau'')G(\tau-\tau'') \tag{15}$$

and $G(\tau-\tau'') = \int_{\tau''}^\tau d\tau'/a(\tau')$. The induced linear density fluctuation δ_{1t} is given by

$$\delta_{1t} = -\mathrm{s}^i_{1t,i} = F(\tau)t^{(0)i}{}_i. \tag{16}$$

The trace of the tidal field t_{ij} is zero, i.e. $\delta_{1t} = 0$, so there is no first order contribution to the density from the tidal field.

The evolution equation for $\mathbf{s}_{2t}$ involves quadratic mixed terms from the coulping between $\mathbf{s}_{1s}$ and $\mathbf{s}_{1t}$. Inserting the Poisson equation[1] to Eq.(6), and subtracting the evolution equations for $\mathbf{s}_{1s}$, $\mathbf{s}_{1t}$ and $\mathbf{s}_{2s}$ leads to

$$\begin{aligned}&\frac{d^2}{d\tau^2}\sigma_{2t} + \mathcal{H}\frac{d}{d\tau}\sigma_{2t} - \frac{3}{2}\Omega_m(\tau)\mathcal{H}^2\sigma_{2t}\\ &= -\frac{3}{2}\Omega_m(\tau)\mathcal{H}^2\delta_{1s}\delta_{1t} + \left(\frac{\partial^i\partial^j}{\nabla^2}\delta_{1s}\right)t_{ij}(\tau),\end{aligned} \tag{17}$$

where $\sigma \equiv \mathrm{s}^i{}_{,i}$. The first term on the right hand of Eq.(17) vanishes since $\delta_{1t} = 0$. This equation can be solved numerically to get

$$\sigma_{2t}(\boldsymbol{q},\tau) = D_{\sigma 1}(\tau)\left(\frac{\partial^i\partial^j}{\nabla^2}\delta_{1s}(\boldsymbol{q},\tau)\right)t^{(0)}_{ij}, \tag{18}$$

where

$$D_{\sigma 1}(\tau) = \int_0^\tau d\tau' \frac{H(\tau)D(\tau') - H(\tau')D(\tau)}{\dot{H}(\tau')D(\tau') - H(\tau')\dot{D}(\tau')}\frac{D^2(\tau')}{D(\tau)a(\tau')} \tag{19}$$

The difference between density contrasts with and without t_{ij} at $\boldsymbol{x}$ is

$$\delta_t(\boldsymbol{x}) = \delta(\boldsymbol{x}) - \delta(\boldsymbol{x})|_{t_{ij}=0}. \tag{20}$$

Since the tidal field induces the displacement $\mathbf{s}_t$ in addition to $\mathbf{s}_s$, the same Lagrangian coordinate $\boldsymbol{q}$ corresponds to different $\boldsymbol{x}$ in these two cases. In the presence of t_{ij}, $\boldsymbol{x} = \boldsymbol{q} + \mathbf{s}_{1s} + \mathbf{s}_{1t}$. Here δ_{1s} solved from linear equations

[1] Note here at linear order $\mathrm{tr}\mathrm{M}_{1t} = -\delta_{1t}$ should not be included when expanding Eq.(10), as it is induced by the long wavelength tidal field t_{ij}, while the coupling between M_{1s} and M_{1t} should be included when expanding to second order as they source the local gravitational potential Φ_s.

gives the density at $\boldsymbol{x}_s = \boldsymbol{q} + \mathbf{s}_{1s} = \boldsymbol{x} - \mathbf{s}_{1t}$. Taking this into account and using Eq.(8), one finally get

$$\delta_t(\boldsymbol{x},\tau) = \delta_{1t}(\boldsymbol{x}) - \sigma_{2t}(\boldsymbol{x}) + \delta_{1t}(x)\delta_{1s}(\boldsymbol{x}) + \mathrm{tr}(\mathrm{M}_{1s}\mathrm{M}_{1t})|_{\boldsymbol{x}} - s^i_{1t}\partial_i\delta_{1s}(\boldsymbol{x}). \quad (21)$$

Inserting first and second order solutions and noting that the tidal field is traceless, we obtain the anisotropic small scale density fluctuations induced by long wavelength tidal field t_{ij}:

$$\delta_t(\boldsymbol{x},\tau) = t^{(0)}_{ij}\left[\alpha(\tau)\frac{\partial^i\partial^j}{\nabla^2} + \beta(\tau)x^i\partial^j\right]\delta_{1s}(\boldsymbol{x},\tau), \quad (22)$$

where $\alpha(\tau) = -D_{\sigma 1}(\tau) + F(\tau)$ and $\beta(\tau) = F(\tau)$.

In the above we have used the linear density-displacement relation $\delta_{1s} = -s^i_{1s,i}$ to derive the small scale density field δ_{1s} from the linear displacement field $\boldsymbol{s}_{1s}$. However, this linear relation does not hold well at low redshifts and small scales [7]. Improvement can be made by adopting the better held logarithmic relation between the divergence of the displacement field and the density field [7],

$$s^{\ i}_{1s,i} = -\ln(1+\delta_{1s}) + \langle\ln(1+\delta_{1s})\rangle, \quad (23)$$

Below we will use the logarithmic variable $\delta_g = \ln(1+\delta_{1s})$ in place of δ_{1s} in the reconstruction. This logarithmic transformation reduces non-Gaussianities in the evolved density field, hence improves the reconstruction [3].

The tidal field t_{ij} with wavenumber k_L can be taken as constant in a small patch with scale $\ll 1/k_L$. Note it is different to have a constant tidal field t_{ij} and a contant gravitational field Φ_L. The former corresponds to the second spatial derivative of the latter. The local correlation function in the free falling frame is

$$\xi(\boldsymbol{r},\tau) = \langle\delta(\mathbf{0},\tau)\delta(\boldsymbol{r},\tau)\rangle, \quad (24)$$

where $\delta = \delta_{1s} + \delta_t$. Using Eq.(22), we obtain

$$\xi(\boldsymbol{r},\tau) = \xi_{1s}(r,\tau) + t^{(0)}_{ij}\left[2\alpha(\tau)\frac{\partial^i\partial^j}{\nabla^2} + \beta(\tau)r^i\partial^j\right]\xi_{1s}(r,\tau), \quad (25)$$

where $\xi_{1s}(r,\tau) = \langle\delta_{1s}(\mathbf{0},\tau)\delta_{1s}(\boldsymbol{r},\tau)\rangle$ is the isotropic linear matter correlation function. The anisotropic distortion of the locally measured small scale density correlation function is induced by the long wavelength tidal field t_{ij}. Transform Eq.(25) to Fourier space, we will get the local tidal distorted power spectrum. We abbreviate k_S as k and suppress the argument k_L since $T(\tau)$ is scale independent, then we finally obtain

$$P(\boldsymbol{k},\tau)|_{t_{ij}} = P_{1s}(k,\tau) + \hat{k}^i\hat{k}^j t^{(0)}_{ij}P_{1s}(k,\tau)f(k,\tau), \quad (26)$$

where $P_{1s}(k,\tau)$ is the undistorted small scale power spectrum, and

$$f(k,\tau) = 2\alpha(\tau) - \beta(\tau)d\ln P_{1s}(k,\tau)/d\ln k. \quad (27)$$

III. TIDAL RECONSTRUCTION

In this section we first obtain the tidal shear estimators, then present the algorithm for density reconstruction.

A. Tidal Shear Estimators

The long wavelength tidal field can be considered as constant if the coherence scale of the small scale density field is much smaller than that of the long wavelength tidal field. We first consider the long wavelength limit, where γ_+ and $\gamma_\times$ are constant in space, then generalize the estimators to the spatial varying case. We also discuss what happens when the long wavelength limit does not hold.

Given the tidal distortion on power spectrum (Eq.26), in the long wavelength limit and under the Gaussian assumption, quadratic shear estimators can be constructed either by using the maximum likelihood method[4] or the inverse variance weighting from galaxy density contrast δ_g [5, 8]:

$$\hat{\gamma}_+ = \frac{1}{Q_{\gamma_+}}\int\frac{d^3k}{(2\pi L)^3}|\delta_g(\boldsymbol{k})|^2\frac{P(k,\tau)}{P^2_{\rm tot}(k,\tau)}f(k,\tau)(\hat{k}_1^2 - \hat{k}_2^2), \quad (28)$$

$$\hat{\gamma}_\times = \frac{1}{Q_{\gamma_\times}}\int\frac{d^3k}{(2\pi L)^3}|\delta_g(\boldsymbol{k})|^2\frac{P(k,\tau)}{P^2_{\rm tot}(k,\tau)}f(k,\tau)(2\hat{k}_1\hat{k}_2), \quad (29)$$

where $P_{\rm tot}(k) = P(k) + P_{\rm N}(k)$ is the observed matter galaxy? power spectrum, and

$$Q_{\gamma_+} = \int\frac{d^3k}{(2\pi)^3}\frac{P^2(k,\tau)}{P^2_{\rm tot}(k,\tau)}f^2(k,\tau)(\hat{k}_1^2 - \hat{k}_2^2)^2, \quad (30)$$

$$Q_{\gamma_\times} = \int\frac{d^3k}{(2\pi)^3}\frac{P^2(k,\tau)}{P^2_{\rm tot}(k,\tau)}f^2(k,\tau)(2\hat{k}_1\hat{k}_2)^2. \quad (31)$$

After integrating over angles in Fourier space, we have

$$Q_{\gamma_+} = Q_{\gamma_\times} = Q = \int\frac{2k^2dk}{15\pi^2}\frac{P^2(k,\tau)}{P^2_{\rm tot}(k,\tau)}f^2(k,\tau) \quad (32)$$

Using Parseval's theorem, we can rewrite the above equations in real space,

$$\hat{\gamma}_+ = \frac{1}{L^3}\int{\rm d}^3x\left[\delta_g^{w_1}(\boldsymbol{x})\delta_g^{w_1}(\boldsymbol{x}) - \delta_g^{w_2}(\boldsymbol{x})\delta_g^{w_2}(\boldsymbol{x})\right], \quad (33)$$

and

$$\hat{\gamma}_\times = \frac{1}{L^3}\int{\rm d}^3x\left[2\delta_g^{w_1}(\boldsymbol{x})\delta_g^{w_2}(\boldsymbol{x})\right], \quad (34)$$

where $\delta_g^{w_1}(\boldsymbol{x})$ and $\delta_g^{w_2}(\boldsymbol{x})$ are two filtered density fields. In Fourier space, they are given by

$$\delta_g^{w_i}(\boldsymbol{k}) = \delta_g(\boldsymbol{k})w_i(\boldsymbol{k}), \quad (35)$$

where

$$w_i(\boldsymbol{k}) = \sqrt{\frac{P(k,\tau)}{QP_{\rm tot}^2(k,\tau)}} f(k,\tau)^{1/2}\hat{k}_i. \quad (36)$$

In deriving Eq.(33) and Eq.(34), we have assumed that the tidal shear field is constant in space. From the expressions for $\hat{\gamma}_+$ and $\hat{\gamma}_\times$, we can see the terms in square brackets give estimates for γ_+ and $\gamma_\times$ at $\boldsymbol{x}$, while the integral $\int d^3x/L^3$ averages the local value over the whole space L^3. If the fluctuation of the tidal field t_{ij} changed on a larger scale than the filtering scale, we can use the localized estimation in the square brackets as estimates for $\gamma_{+,\times}$ [4, 5, 8]. The unbiased minimum variance estimates of the spatial varying tidal field in the long wavelength limit is given by

$$\begin{aligned}\hat{\gamma}_+(\boldsymbol{x}) &= \left[\delta_g^{w_1}(\boldsymbol{x})\delta_g^{w_1}(\boldsymbol{x}) - \delta_g^{w_2}(\boldsymbol{x})\delta_g^{w_2}(\boldsymbol{x})\right],\\ \hat{\gamma}_\times(\boldsymbol{x}) &= \left[2\delta_g^{w_1}(\boldsymbol{x})\delta_g^{w_2}(\boldsymbol{x})\right]. \end{aligned} \quad (37)$$

The estimators given in Eq.(37) were derived assuming that compared with the small scale density field, the long wavelength tidal shear fields vary slowly. If this long wavelength limit is not satisfied, the tidal shear reconstruction would be biased by a multiplicative bias factor $b(\boldsymbol{k})$, which approaches to unity in the limit $k \to 0$ and decreases when k increases [4, 8]. In the cosmic tidal reconstruction, we mainly use the nonlinear structures around the scale 1.25 Mpc/h to reconstruct the long wavelength tidal field [3], so for the reconstructed large scale density perturbations with wavenumber $k_L \lesssim 0.1\ h$/Mpc we can ignore this multiplicative bias.

B. Density Reconstruction Algorithm

The tensor field $\Phi_{L,ij}$ has six components. Such symmetric 3×3 tensor can be decomposed into 6 orthogonal components [6, 9], i.e. $\Phi_{L,ij} = A_a\epsilon^a_{ij}$, where A_a is the expansion coefficient and ϵ^a_{ij} statisfies the orthogonal relation $\epsilon^a_{ij}\epsilon^{bji} \propto \delta^{ab}$. We decompose $\Phi_{L,ij}$ as

$$\Phi_{L,ij} = (1+\epsilon_0)\delta_{ij} + t_{ij}, \quad (38)$$

where $\epsilon_0 = \nabla^2\Phi_L/3$, $\gamma_+ = (\Phi_{L,11}-\Phi_{L,22})/2$, $\gamma_\times = \Phi_{L,12}$, $\epsilon_x = \Phi_{L,13}$, $\epsilon_y = \Phi_{L,23}$, and $\epsilon_z = (2\Phi_{L,33} - \Phi_{L,11} - \Phi_{L,22})/6$. Here the tensor is decomposed in a way such that when reduced to the 2D case, notations reduce to those used in gravitational lensing, so the z axis plays a different role than the $x-$ and $y-$axes. For intuitive unsterdandings of these abstract symbols, see the figures in [6]. All these 6 different components will induce different observable effects in the local quadratic statistics, including the isotropic modulations (ϵ_0) and anisotropic parts (γ_+, $\gamma_\times$, etc). The large scale gravitational potential Φ_L is a single number, so it is six fold overdetermined. Li et al.[2] used the isotropic modulation to reconstruct the large scale density field. Here we focus on the "change of shape", i.e. the traceless tidal field $t_{ij} = \Phi_{L,ij} - \nabla^2\Phi_L\delta_{ij}/3$ instead.

The induced local anisotrpy pattern by long wavelength tidal field is proportional to t_{ij}. Using orthogonal components introduced above, Eq.(26) can be written as

$$\frac{\delta P(\boldsymbol{k},\tau)|_{t_{ij}}}{P_{1s}(k,\tau)} = f(k,\tau)[(\hat{k}_1^2 - \hat{k}_2^2)\gamma_+^{(0)} + 2\hat{k}_1\hat{k}_2\gamma_\times^{(0)}] + \cdots \quad (39)$$

Here we only write out the γ_+ and $\gamma_\times$ terms explicitly. The distortion along the l.o.s. (i.e. the z-direction in the above coordinates) is not available in imaging-only surveys, and even for spectroscopic surveys, it is often affected by peculiar velocities and not precisely known, so here we shall use γ_+ and $\gamma_\times$ which only involve derivatives in the tangential $x-y$ plane. In the language of weak lensing, γ_+ and $\gamma_\times$ describe quadrapolar distortions of in the $x-y$ plane. Peculiar velocities cause particles moving along z axis, but we expect the changes in γ_+ and $\gamma_\times$ due to peculiar velocities would be a second order effect.

We can convert the tidal shear field γ_+ and $\gamma_\times$ into the "convergence" field $\kappa_{\rm 2D} = (\Phi_{L,11} - \Phi_{L,22})/2$ as in gravitational lensing [10], $\kappa_{\rm 2D,11}+\kappa_{\rm 2D,22} = \gamma_{+,11}-\gamma_{+,22}+2\gamma_{\times,12}$. In Fourier space, it can be written as

$$\kappa_{\rm 2D}(\boldsymbol{k}) = \frac{1}{k_1^2+k_2^2}[(k_1^2-k_2^2)\gamma_+(\boldsymbol{k}) + 2k_1k_2\gamma_\times(\boldsymbol{k})]. \quad (40)$$

where we use the subscript 2D to indicate that κ_{2D} is the 2D "convergence" field in a constant redshift slice. It can be converted into the "convergence" field in three dimensional $\kappa_{\rm 3D} = \nabla^2\Phi_L$ as

$$\begin{aligned}\kappa_{\rm 3D}(\boldsymbol{k}) &= \frac{2k^2}{k_1^2+k_2^2}\kappa_{\rm 2D}(\boldsymbol{k}) \\ &= \frac{2k^2}{(k_1^2+k_2^2)^2}[(k_1^2-k_2^2)\gamma_+(\boldsymbol{k}) + 2k_1k_2\gamma_\times(\boldsymbol{k})].\end{aligned} \quad (41)$$

Now we get an estimate of the large scale density field by measuring γ_+ and $\gamma_\times$. The large scale density field δ_L only differs from $\kappa_{\rm 3D}$ by a constant factor which we will address in a moment.

Note that this reconstruction is inherently 3D instead of 2D. As only γ_+ and $\gamma_\times$ are used, one might thought that the cosmic tidal reconstruction takes place in different 2D slices with constant redshifts. However, although γ_+ and $\gamma_\times$ only involve derivatives in the tangential plane, the changes of γ_+ and $\gamma_\times$ along z axis encode the change of δ_L along z axis. Since we only use $\gamma_{+,\times}$ instead of all components in the tidal field t_{ij} for reconstruction, the error of the reconstructed mode $\kappa_{\rm 3D}(\boldsymbol{k})$ is anisotropic in $\boldsymbol{k}$. The variance of $\kappa_{\rm 3D}(\boldsymbol{k})$ is

$$\begin{aligned}\langle\kappa_{\rm 3D}(\boldsymbol{k})\kappa_{\rm 3D}(\boldsymbol{k}')\rangle &= \big[(k_1^2-k_2^2)({k'_1}^2-{k'_2}^2)\langle\gamma_+(\boldsymbol{k})\gamma_+(\boldsymbol{k}')\rangle \\ &+(2k_1k_2)(2k'_1k'_2)\langle\gamma_\times(\boldsymbol{k})\gamma_\times(\boldsymbol{k}')\rangle\big] \times \frac{2k^2}{(k_\perp^2)^2}\frac{2{k'}^2}{({k'_\perp}^2)^2}, \end{aligned} \quad (42)$$

where $k_\perp = k_1^2 + k_2^2$. How is this derived? It is not very obvious The power spectrum of $\gamma_{+,\times}$ is scale independent on large scales [11], so

$$\langle\kappa_{3D}(\boldsymbol{k})\kappa_{3D}(\boldsymbol{k}')\rangle \propto [(k_1^2-k_2^2)(k_1'^2-k_2'^2)+(2k_1k_2)(2k_1'k_2')] \times\frac{2k^2}{(k_\perp^2)^2}\frac{2k'^2}{(k_\perp'^2)^2}\delta^D(\boldsymbol{k}+\boldsymbol{k}'), \quad (43)$$

where $\delta^D(\boldsymbol{k})$ is the Dirac delta function. The error in the reconstructed mode $\kappa_{3D}(\boldsymbol{k})$ is given by derivation?

$$\sigma^2_{\kappa_{3D}} \propto \left(\frac{k^2}{k_\perp^2}\right)^2. \quad (44)$$

If we could include the z components the error would be isotropic, but redshift space distortion will influence the reconstruction. This will be investigated in the future.

From Eq.(44) we see that when $k_\perp \to 0$ the error is infinite for the corresponding $\kappa_{3D}(\boldsymbol{k})$. In this case, the estimator in Eq.(41) diverges. As these modes contain nothing but noise, we set these modes to zero in our reconstruction. Since the error varies for modes with different $k_\perp$ and $k_\parallel$, we need to filter the reconstructed density field κ_{3D} to obtain the clean density field κ.

In general, the reconstructed noisy 3D convergence field κ_{3D} is related to the original density field by

$$\kappa_{3D}(k_\parallel,k_\perp) = b(k_\parallel,k_\perp)\delta_L(k_\parallel,k_\perp)+n(k_\parallel,k_\perp), \quad (45)$$

where $b(k_\parallel,k_\perp)$ is the bias factor and $n(k_\parallel,k_\perp)$ is the noise in reconstruction. The bias factor and the noise can be determined from the cross correlation of κ_{3D} and the original density field δ and the auto-correlation function of κ_{3D},

$$\begin{aligned}\langle\kappa_{3D}\delta\rangle &= b\langle\delta\delta\rangle,\\ \langle\kappa_{3D}\kappa_{3D}\rangle &= b^2\langle\delta\delta\rangle+\langle nn\rangle.\end{aligned} \quad (46)$$

We then get

$$b(k_\parallel,k_\perp) = \frac{P_{\kappa_{3D}\delta}(k_\parallel,k_\perp)}{P_{\delta\delta}(k_\parallel,k_\perp)} \quad (47)$$

and

$$P_{\kappa_{3D}}(k_\parallel,k_\perp) = b^2(k_\parallel,k_\perp)P_{\delta\delta}(k_\parallel,k_\perp)+P_n(k_\parallel,k_\perp). \quad (48)$$

We correct the bias factor and apply the Wiener filter to obtain the reconstructed field $\hat\kappa$ which we use as the estimator of δ,

$$\hat\kappa(k_\parallel,k_\perp) = \frac{W(k_\parallel,k_\perp)}{b(k_\parallel,k_\perp)}\kappa_{3D}(k_\parallel,k_\perp), \quad (49)$$

where

$$W(k_\parallel,k_\perp) = \frac{P_{\delta\delta}(k_\parallel,k_\perp)}{P_{\delta\delta}(k_\parallel,k_\perp)+P_n(k_\parallel,k_\perp)/b^2(k_\parallel,k_\perp)}, \quad (50)$$

The real space $\hat\kappa(x)$ can then be obtained by inverse Fourier transformation.

IV. SIMULATION

Now we make a complete simulation of the cosmic tidal reconstruction process with all the details. For this purpose, we run N-body simulations with 2048^3 dark matter particles in a box of side length $L = 1.2$ Gpc$/h$, with $\Omega_b = 0.049$, $\Omega_b = 0.259$, $h = 0.678$, $A_s = 2.139\times10^{-9}$ and $n_s = 0.968$. Six simulations with independent initial conditions are run to provide better statistics. The computation is performed on BlueGene/Q supercomputer located at the University of Toronto's SciNet HPC facility, using the CUBEP^{3}M [12].

A. Reconstruction

We will follow the simple, slightly sub-optimal scenario in [3]. We first smooth 3D density field using a Gaussian window

$$\bar\delta(\boldsymbol{x}) = \int d^3x' S(\boldsymbol{x}-\boldsymbol{x'})\delta(\boldsymbol{x}'), \quad (51)$$

where $S(\boldsymbol{r}) = e^{-r^2/2R^2}$. We need to remove high density peaks from the density field since the quadratic estimator heavily weights the high density regions. What do you mean remove the high density peak? Is it the smoothing operation or is it an additional operation? We choose the smoothing scale $R = 1.25$Mpc$/h$ as in [3] need add some reason. We will also show below that the reconstruction result is not sensitive to the smoothing scale as long as the scale is in the nonlinear regime, i.e. $R \gtrsim 5$Mpc$/h$. After the smoothing, we take a logarithmic transform

$$\delta_g(\boldsymbol{x}) = \ln[1+\bar\delta(\boldsymbol{x})] \quad (52)$$

to Gaussianize the non-Gaussian (smoothed) density field as motivated by [7]. The additive constant $\langle\ln(1+\bar\delta(\boldsymbol{x}))\rangle$ does not affect our reconstruction results, as we only need the derivatives of this field.

Next we convolve the log density field $\delta_g(\boldsymbol{x})$ with the filter $w_i(\boldsymbol{x})$ in Eq.(36), and then obtain the three dimensional tidal shear fields $\gamma_+(\boldsymbol{x})$ and $\gamma_\times(\boldsymbol{x})$ using Eq.(37). The quadrupolar distortions of the density field in the tangential plane are shown by the two tidal shear fields $\gamma_+(\boldsymbol{x})$ and $\gamma_\times(\boldsymbol{x})$ directly, while the variation along the z axis can be inferred from the variation of the tidal shear field in the z direction.

Finally by combining $\gamma_+(\boldsymbol{k})$ and $\gamma_\times(\boldsymbol{k})$ using Eq.(41), we obtain the 3D "convergence" field $\kappa_{3D}(\boldsymbol{k})$. We estimate $\langle\kappa_{3D}\delta\rangle$ and $\langle\kappa_{3D}\kappa_{3D}\rangle$ using the power spectra from these six simulations, and estimate the final $\hat\kappa(\boldsymbol{k})$ from Eq.(49).

In Fig. 1, we show a 1.17 Mpc$/h$ slice of one of the simulations. The original density field in the $x-y$ plane is shown in the left panel and a slice of the reconstructed density field is shown in the right panel, both smoothed on 8 Mpc$/h$ to reduce the small scale noise in order to make visual comparisons. We also show in Fig. 2 a slice

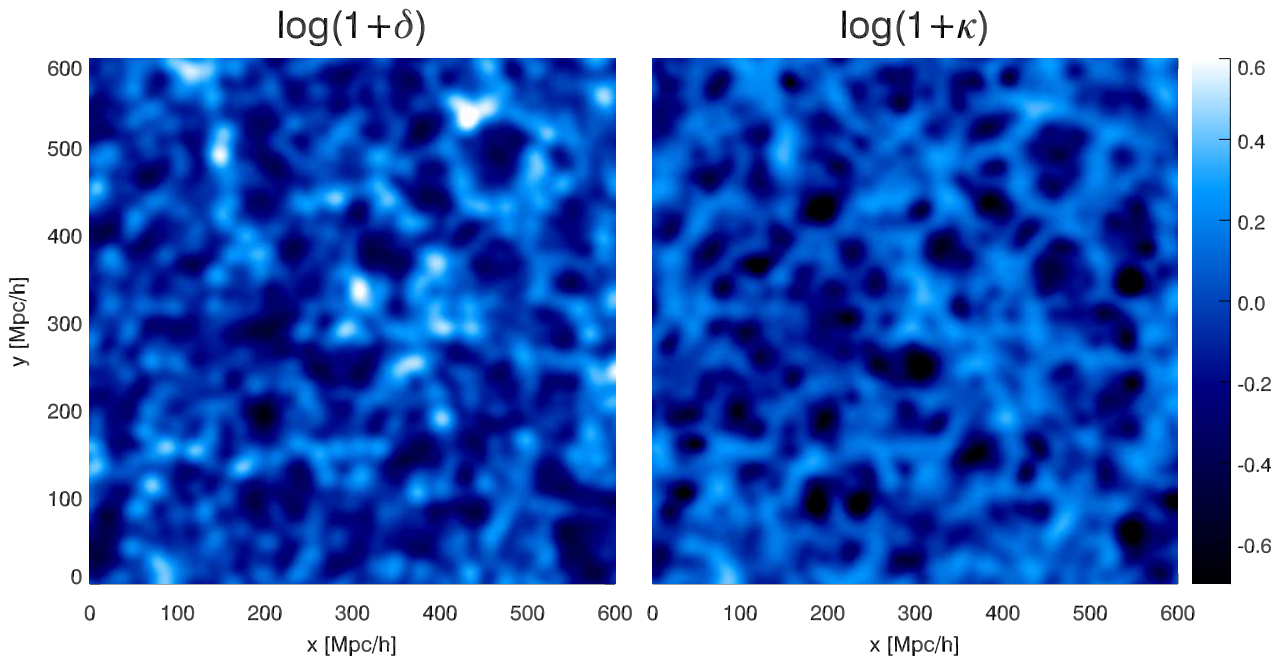

FIG. 1: The left panel shows a slice of the original density field $\delta(\boldsymbol{x})$ smoothed on 8 Mpc/h in $x-y$ plane. The right panel shows the corresponding slice of the reconstructed density field $\kappa(\boldsymbol{x})$, also smoothed on 8 Mpc/h.

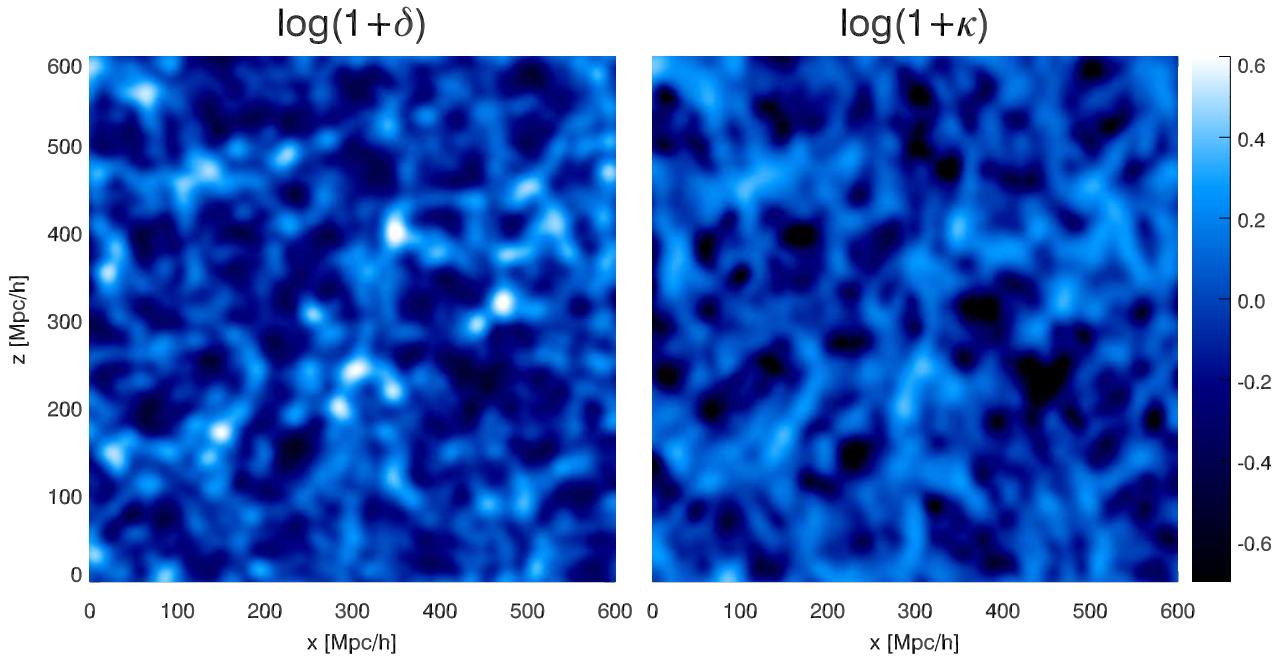

FIG. 2: The left panel shows a slice of the original density field $\delta(\boldsymbol{x})$ smoothed on 8 Mpc/h in $x-z$ plane. The right panel shows the corresponding slice of the reconstructed density field $\kappa(\boldsymbol{x})$, also smoothed on 8 Mpc/h.

of the density field in the $x-z$ plane. We find that in both the $x-y$ and $x-z$ plane, the reconstructed density field is very similar to the original one, showing that the reconstruction results are good. However, the strong peaks in the original density field are much less prominent in the reconstructed field.Isn't this the result of smoothing? The peaks in the original density field correspond to strongly nonlinear structures, such as some very massive halos. The gravitational self-interaction is very strong around such structures. The local anisotropic features arising from the large scale tidal field is relatively small compared to that from the gravitational self-interaction in these regions. Eq.(26) may not hold in these regimes. This may be the reason why the cosmic tidal reconstruc-

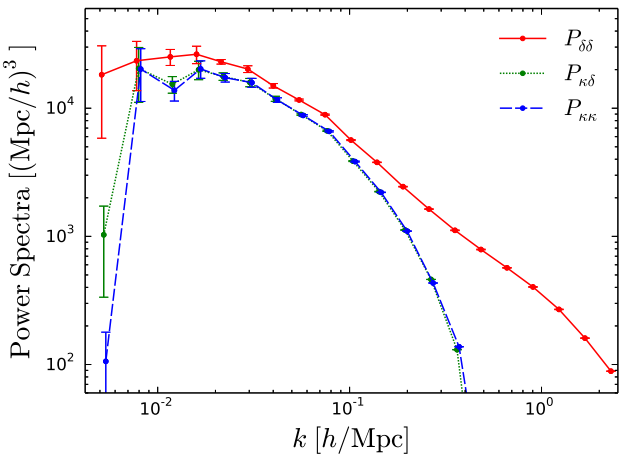

FIG. 3: Power spectra for different fields. The red solid line shows the power spectrum of the original density field $\delta(\boldsymbol{x})$. The green dotted line shows the cross power spectrum of the original density field and the reconstructed density field $\kappa(\boldsymbol{x})$. The blue dashed line shows the power spectrum of the reconstructed density field $\kappa(\boldsymbol{x})$.

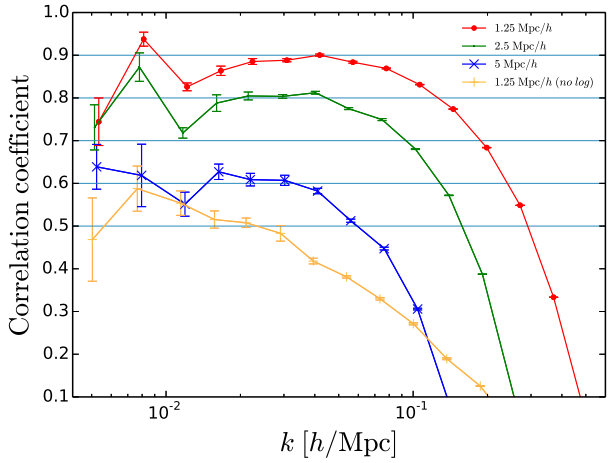

FIG. 4: Cross correlation coefficients for different smoothing lengths and the reconstruction without applying logarithmic transformation.

tion does not recover these peaks. ue-li are you satisfied with this explanation? Could you check whether the peak "disappeared", or merely less prominent? My impression is that it may be the later case.

The cross-correlation between the reconstructed field and the original field shows quantitatively how well is the reconstruction. In Fig. 3, we show the auto power spectra of the original field δ, the reconstructed field κ and the cross power spectrum of the two, Data points of the three spectra in the same k-bin are shifted slightly for clarity of display. We see a good cross correlation between the original and the reconstructed density fields over a wide range in wave numbers. The power spectrum for κ and the cross power spectrum between κ and δ are almost the same. In Fig. 4 we plot the cross correlation coefficient, which is defined as $r_{\kappa\delta} \equiv P_{\kappa\delta}/\sqrt{P_{\delta\delta}P_{\kappa\kappa}}$. The error bars are estimated by the Bootstrap resampling method. For our fiducial case where a smoothing scale of 1.25Mpc$/h$ is used, the correlation coefficient is above 0.8 for $k \lesssim 0.1$ Mpc$/h$, and is close to 0.9 at some scales.

B. Dependence on Smoothing Scale and Gaussianization

To test how does the reconstruction result depends on the choice of smoothing scale, we also performed reconstruction with two more smoothing scales, $R = 2.5$ Mpc$/h$ and $R = 5$ Mpc$/h$. Fig. 4 shows the cross correlation coefficients for all these three cases. We see that the cross correlation coefficient decreases when the smoothing scales are increased. This is expected: the information encoded in the anisotropic small scale structures are used to reconstruct the large scale density field, with large smoothing length, some information hidden in the small scale structures are lost, resulting low signal-to-noise ratio in the reconstructed field. However, the reconstruction results do not degrade significantly until the smoothing scale goes beyond 5 Mpc$/h$, which is also roughly the scale on which the structure growth transits from linear to non-linear, so the reconstruction is not sensitive to the smoothing scale unless we smooth on the linear scales. The scale 5 Mpc/h is roughly the nonlinear scale, but I am not too sure if this degradation is really due to non-linearity, or it is merely a problem with limited available modes. Judging from the shape, the latter seems likely. Need to check this, either with analytical formula, or by some kind of test, e.g. in the finer resolution case, only use a fraction of the modes for reconstruction.

The logarithmic transform plays an important role in cosmic tidal reconstruction. In Figure 4 we also plot the result for a reconstruction without the logarithmic transform. We find the cross correlation between the reconstructed field and the original field is much weaker than the one obtained with logarithmic transformation, and quickly drops to nearly zero when the wavenumber increases. Apparently, in this case the non-Gaussianity developed in the density field impaired the accuracy of the shear reconstruction. The tidal shear estimators derived with the Gaussian assumption are not necessarily optimal for the non-Gaussian case. However, the logarithmic transform captures a large part of the non-linear evolution, it also fixes the displacement-density relation significantly as shown in [7], so the logarithmic transformation greatly reduces the non-Gaussianity of the density field, allowing much better result to be achieved. is this argument good??

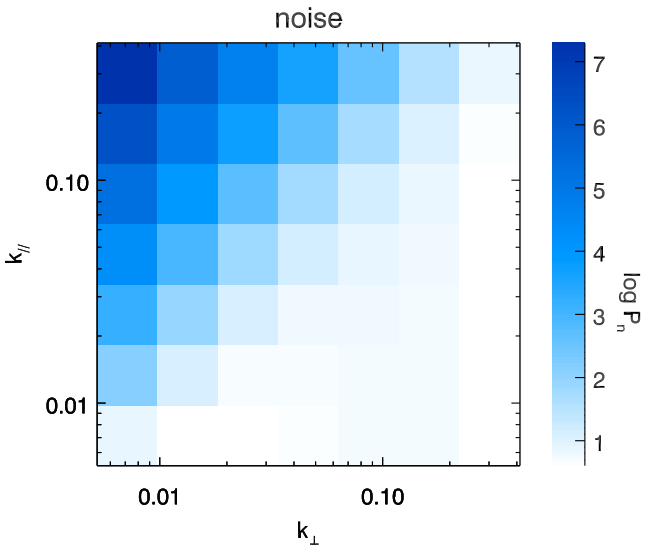

FIG. 5: The anisotropic noise power spectrum $P_n(k_\parallel, k_\perp)$.

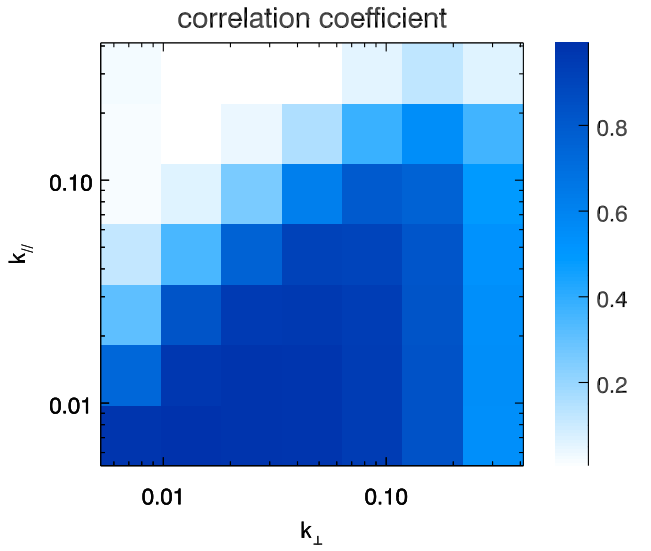

FIG. 6: The anisotropic cross correlation coefficient $r_{\kappa\delta}(k_\parallel, k_\perp)$.

C. The Anisotropic Noise

For the reconstruction described above, the error in κ_{3D} is anisotropic as we discussed earlier. We show the anisotropic noise power spectrum in Fig. 5. The noises for modes with large $k_\parallel$ and small $k_\perp$ are orders of magnitude larger than other modes. This result confirms the estimate of noise derived from theory, $\sigma_{\kappa_{3D}} \propto k^2/k_\perp^2$, which diverges for small $k_\perp$. In Fig. 6, we show the anisotropic correlation coefficient $r_{\kappa\delta}(k_\parallel, k_\perp) = P_{\kappa\delta}(k_\parallel, k_\perp)/\sqrt{P_{\delta\delta}(k_\parallel, k_\perp)P_{\kappa\kappa}(k_\parallel, k_\perp)}$. The correlation between the original and the reconstructed field is better at the lower right corner, which could be close to 1 for modes with large $k_\perp$, but drops to 0 quickly when $k_\parallel$ increases, the modes with large $k_\parallel$ and small $k_\perp$ are poorly reconstructed.

In Fig. 7 we show the anisotropic bias factor, which is almost scale independent, except for modes with very large $k_\parallel$ and very small $k_\perp$, where the cosmic tidal reconstruction failed.

Such anisotropy in reconstruction is due to the fact we only use tidal shear fields in the $x-y$ plane to reconstructed the long wavelength density field. The changes of the long wavelength density field δ_L are inferred from the variation of tidal shear fields $\gamma_+(\boldsymbol{x})$ and $\gamma_\times(\boldsymbol{x})$ along z axis, i.e. we reconstruct these modes indirectly, so we can not capture rapid changes of the density field along z axis. By including tidal shear fields containing derivatives with respect to z axis, the reconstruction may be improved. However, accurate radial direction measurement requires more observing resources, and in any case redshift space distortion will inevitably affect the reconstruction result. We leave the detailed study of this in a future paper.

V. DISCUSSIONS

In this paper we studied the tidal distortions of long wavelength perturbations on the small scale perturbations, and showed how the long wavelength perturbation can be reconstructed from the small scale anisotropic perturbations. We considered the tidal distortions which are proportional to $\hat{k}^i\hat{k}^j t_{ij}^{(0)}$, and assumed that the proportional coefficient varies slowly over different wave numbers. We can absorb the unknown coefficient into the bias factor introduced in Eq.(45), then measure it with N-body simulations. The proportional constant from the Poisson equation which? and the normalization constant Q in the tidal shear estimators can also be absorbed in this bias factor. The integral for Q in Eq.(32) would diverge at large k if there were no noise in the power spectrum $P(k)$, i.e. $P(k) = P_{tot}(k)$, as happens when we use the dark matter density field from high precision N-body simulations to reconstruct the large scale density field. The bias factor solves this problem.I am a bit confused by this point, more explanation? Also, this discussion can be put right after Eq.(32) .

Here we considered the leading order effect, i.e. the coupling between $\mathbf{s}_{1s}$ and $\mathbf{s}_{1t}$. Higher order terms of the form $(\mathbf{s}_{1s})^n\mathbf{s}_{1t}$ with $(n > 1)$ may also make significant contribution, as the nonlinearities on small scales are quite strong. The proportional coefficient $f(k,\tau)$ in Eq.(26) will be changed if such higher order terms are included. The result could be improved in the future by including the higher order perturbations. Nevertheless, he reconstruction is well performed , with the cross correlation coefficient larger than 0.8 until $k \gtrsim 0.1\mathrm{Mpc}/h$ and on some scales close to 0.9. The reconstruction should work even better at higher redshifts where the small scale density fluctuations undergo less nonlinear evolution.

The $\hat{\gamma}_+$ and $\hat{\gamma}_\times$ estimators are unbiased and of min-

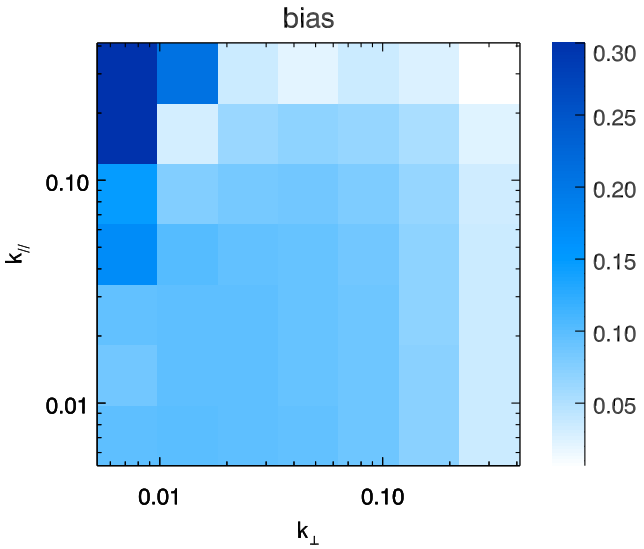

FIG. 7: 2D bias factor $b(k_\parallel, k_\perp)$. The bias factor is almost scale independent in this plane. $b(k_\parallel, k_\perp)$ saturates at the upper left corner. Since these modes are noisy, the extremely large values of the bias at that corner are not reliable.

imum variance in the long wavelength limit, providing optimal tidal shear reconstructions. However, at larger wavenumbers, the tidal shear fields would be underestimated by a scale dependent bias factor which need to be corrected. The estimator derived in the long wavelength limit still works well if we only use the reconstruction modes with scale larger than the smoothing scale. However, when there is an overlap between these two scales, the reconstruction result would degrade. More sophisticated method is needed in that case. Also, the estimators we derived in this paper are optimal under the Gaussian assumption, but in reality the nonlinear density field is not Gaussian. The logarithmic transformation helps to Gaussianize the non-Gaussian density field and as a result we still get pretty good result. It would be worthwhile to investigate the optimal estimators for non-Gaussian sources, which can be constructed from N-body simulations. Finally, here we use the dark matter density field directly to reconstructed the large scale density field. However, galaxies and halos are distributed in the underlying dark matter density field. Due to the discreteness of the galaxy/halo field, the tidal reconstruction may not be as good as that of the dark matter field. The scale dependent galaxy/halo bias may also complicate the reconstruction. We plan to study this in future.

The reconstruction method developed in this paper has many applications. For example, the reconstructed field κ gives the distribution of dark matter on large scales, by cross correlating with the original galaxy/halo field, we could measure the logrithmic growth rate without sample variance [13]. This potentially gives precision measurements of neutrino masses and tests of gravity. Moreover, it can also be applied to the case where the measurement of longwave mode is missing, for example the data obtained with the 21cm intensity mapping survey. In 21cm intensity mapping surveys, modes with small radial wavenumber is contaminated by foreground radiation and is often subtracted in data analysis, which makes it impossible to do cross-correlation with surveys which provide only long mode measurement, such as the measurements made with weak lensing tomography, photo-z galaxies, integrated Sachs-Wolf effect and kinematic Sunyaev Zel'dovich effect. Since cosmic tidal reconstruction can recover these long wavelength modes from small scale modes, it would enable us to reconstruct the long wavelength modes from 21cm intensity mapping data, which can be used to cross correlate with the other cosmic probes. This is be investigated in another paper But there are some problems in this arguement. The method given here would be useful in reconstructing density modes, but not useful to reconstruct 21cm modes. The 21cm modes also include the effect of ionization fraction and spin temperature, which can not be recovered from this reconstruction. When people do the cross-correlation they are usally trying to look for these effects, not the density modes.

Finally, the tidal reconstruction will be useful in the study of 21cm lensing, where distant 21cm signal are used as the source for lensing. The nonlinearity in the 21cm temperature field limits the precision of lensing reconstruction [4, 5]. However, the tidal interaction is also responsible for the local quadrupole distortions, so we could use the large scale density to remove the tidal distortions to reduce the nonlinearities in the observed 21cm temperature field, just like BAO reconstruction. This will improve 21cm lensing significantly.

VI. ACKNOWLEDGEMENT

We acknowledge the support of the Chinese MoST 863 program under Grant No. 2012AA121701, the CAS Science Strategic Priority Research Program XDB09000000, the NSFC under Grant No. 11373030, Tsinghua University, CHEP at Peking University, and NSERC. X. Er is supported by the NSFC under Grant No. 11473032.

[1] F. Schmidt, E. Pajer, and M. Zaldarriaga, Phys. Rev. D **89**, 083507 (2014), 1312.5616.
[2] Y. Li, W. Hu, and M. Takada, Phys. Rev. D **90**, 103530 (2014), 1408.1081.
[3] U.-L. Pen, R. Sheth, J. Harnois-Deraps, X. Chen, and Z. Li, ArXiv e-prints (2012), 1202.5804.
[4] T. Lu and U.-L. Pen, MNRAS **388**, 1819 (2008), 0710.1108.

[5] T. Lu, U.-L. Pen, and O. Doré, Phys. Rev. D **81**, 123015 (2010), 0905.0499.
[6] D. Jeong and M. Kamionkowski, Physical Review Letters **108**, 251301 (2012), 1203.0302.
[7] B. L. Falck, M. C. Neyrinck, M. A. Aragon-Calvo, G. Lavaux, and A. S. Szalay, ApJ **745**, 17 (2012), 1111.4466.
[8] M. Bucher, C. S. Carvalho, K. Moodley, and M. Remazeilles, Phys. Rev. D **85**, 043016 (2012), 1004.3285.
[9] D. M. Eardley, D. L. Lee, A. P. Lightman, R. V. Wagoner, and C. M. Will, Physical Review Letters **30**, 884 (1973).
[10] N. Kaiser and G. Squires, ApJ **404**, 441 (1993).
[11] M. Zaldarriaga and U. Seljak, Phys. Rev. D **59**, 123507 (1999), astro-ph/9810257.
[12] J. Harnois-Déraps, U.-L. Pen, I. T. Iliev, H. Merz, J. D. Emberson, and V. Desjacques, MNRAS **436**, 540 (2013), 1208.5098.
[13] P. McDonald and U. Seljak, J. Cosmology Astropart. Phys. **10**, 007 (2009), 0810.0323.